A Warming Structure for Piezoelectric Stack Working in Cryogenic Temperature

LIN Yufan[1], *QIN Xuguo*[2], *YU Yi*[1], *FAN Siyun*[1], *SHEN Xing*[1*]

1. State Key Laboratory of Mechanics and Control of Mechanical Structures, Nanjing University of Aeronautics and Astronautics, Nanjing 210016, P. R. China;
2. Beijing Institute of Space Long March Vehicle, Beijing 100076, P. R. China

(Received 17 March 2020; revised 20 April 2020; accepted 8 May 2020)

Abstract: It is widely acknowledged that the performance of a piezoelectric stack would decline with the temperature decreasing, which will exert negative influence on its application in low-temperature environment. Therefore, a convenient and efficient warming structure for the piezoelectric stack is proposed in this paper to solve this problem. Based on the theoretical analysis of heat transfer, two heating modes, namely, overall heating and local heating are analyzed and compared. Moreover, experimental tests are conducted to evaluate the effectiveness of the structure. Based on the results, it can be concluded that the theoretical results are confirmed with experimental results. Besides, the temperature and performance of the piezoelectric stack are kept stable as temperature varies from 10 ℃ to −70 ℃, which manifests the feasibility of the structure. Therefore, this paper could be an available reference for those engaged in cryogenic investigation of smart materials and structures.

Key words: warming structure; piezoelectric stack; cryogenic temperature; heat transfer

CLC number: TB381;TB941 **Document code:** A **Article ID:** 1005-1120(2020)05-0713-13

0 Introduction

Piezoelectric stack actuators have superior electromechanical coupling characteristics, fast response and large output force[1-4], and thus they are widely employed in precise actuation, micro-positioning systems, active vibration control of the sting used in wind tunnel, vibration isolation system of helicopter and non-destructive evaluation, etc[5-9]. In recent years, piezoelectric stacks have been extensively used in extreme environments such as high temperature, vacuum and radiation, of which cryogenic temperature applications are the most exemplified cases[10]. For example, the piezoelectric stack is put to use for the purpose of active vibration control of the cantilever sting in the cryogenic wind tunnel[11-13], where the ambient temperature would drop to −150 ℃. It is worth mentioning that the temperature drop will directly affect the properties, output characteristics and driving load capability of a piezoelectric stack, resulting in the degradation of working efficiency[14-16]. This phenomenon results from piezoelectric ceramic material composition, dopants, grain size and internal defects, and is dependent on the change of temperature[17]. Hence, as for applications in low temperature environment, feasible warm-maintaining measures are required to keep the temperature at room temperature to ensure the working performance of the stack. On the other hand, piezoelectric stacks generate heat after running for a long time under high frequencies or high electric field magnitudes[18]. Up to now, the majority of the current research lays emphasis on the design and testing of the heat dissipation structures for the piezoelectric transformers, but the heating and insulation struc-

*Corresponding author, E-mail address: shenx@nuaa.edu.cn.

How to cite this article: LIN Yufan, QIN Xuguo, YU Yi, et al. A warming structure for piezoelectric stack working in cryogenic temperature[J]. Transactions of Nanjing University of Aeronautics and Astronautics, 2020, 37(5): 713-725.

http://dx.doi.org/10.16356/j.1005-1120.2020.05.006

tures for the piezoelectric stacks have been rarely studied. Rivers et al. conducted a preliminary study in the cryogenic wind tunnel, but the internal heating of the piezoelectric device turned out to be unsuccessful, and thus they designed and applied a new heating system for the recent low temperature tests. Their results indicated that the damper piezoelectric elements were kept at room temperature when the out temperature was −150 ℃[19]. However, there is a lack of details or working principles about the heating system. For the purpose of ensuring the normal performance of the piezoelectric stack in cryogenic environment, it is highly significant and necessary to keep the piezoelectric stack working at appropriate temperature.

In this paper, a simple and effective insulation structure is presented on the basis of theoretical analysis and experiments. In accordance with the theoretical analysis of the axial heat conduction of the piezoelectric stack, the temperature distributions of the stack in the axial direction under two different heating modes-overall heating and local heating are compared. Furthermore, experimental tests are carried out under local heating conditions to evaluate the thermal insulation effect of the structure.

1 Structural Design and Theoretical Analysis

1.1 Structural design

According to previous study, it can only be heated and insulated in the radial direction of the piezoelectric stack for the reason that the two ends of the stack are directly installed to the mechanical structure to transfer the force. The schematic of the heating and insulation structure is shown in Fig.1. As can be seen, the heating film is attached to the outer surface of the piezoelectric stack with the packaging housing, and then the outside of the heating film is wrapped with the heat insulation materials. Moreover, the entire structure is installed in the mechanical structure, which is exposed to cryogenic environment.

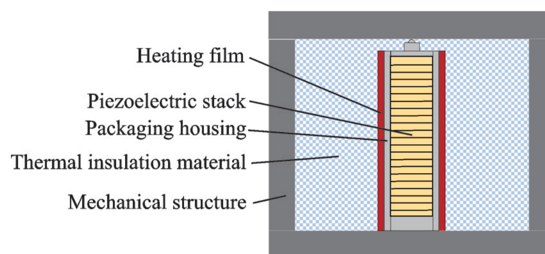

Fig.1 Schematic diagram of the heating and insulation structure

1.2 Theoretical analysis

Energy generated by the heating film leads to a rise in the temperature of the stack, and since the insulating effect merely exists in the radial direction, energy is mainly transferred in the axial direction. According to the heat transfer theory, when a steady state is reached, the heat generated per unit time is equal to the heat dissipated by external heat conduction, which means the generated heat and released heat reach a thermal equilibrium. That is to say, if the temperature of the piezoelectric stack can be stably maintained at normal temperature, the structure can be regarded as effective.

1.2.1 Overall heating theoretical analysis

The outer surface of the piezoelectric stack with the packaging housing is integrally attached with a heating film, which belongs to the overall heating theoretical model. For the convenience of analysis, the layer of insulating material is regarded as an adiabatic boundary, and thus all the energy generated is transferred to the package housing as well as the piezoelectric stack in turn. Subsequently, the heat is transferred along the axial direction of the stack. The hemispherical top of the packaging housing is linked to the mechanical structure by means of point contact. Hence, the top is considered to be an adiabatic boundary as well, indicating that the entire energy can only be transferred to the external environment by way of the bottom of the stack. The schematic diagram of the overall heating conduction model is shown in Fig.2.

In accordance with heat conduction theory, relevant studies of geometric effects, material properties as well as boundary conditions, the two- or

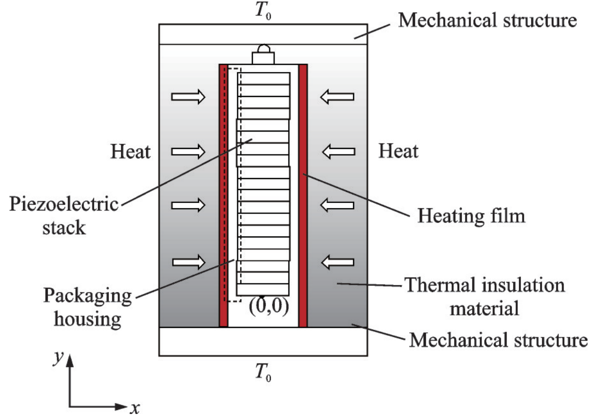

Fig.2 Whole heating thermal conductivity model

three-dimensional heat conduction model can be reasonably simplified into a one-dimensional heat conduction model[20]. A piezoelectric stack with a packaging housing can be deemed as a cylindrical member, and consequently the thermal conduction in the radial direction is the steady-state heat conduction of the composite cylinder, while that in the axial direction is the steady-state heat conduction of the multi-layer plate. As the consequence, in line with the concept of thermal resistance, the thermal resistances of the piezoelectric stack in the radial (x direction) R_x and the axial (y direction) R_y[21] can be calculated and compared. To be specific, the radial thermal resistance can be calculated from $r_1 = 1$ mm in the radial direction to the package housing radius $r_f = 7.5$ mm as follows

$$R_x = \frac{1}{2\pi l_p}\left(\frac{\ln(r_p/r_1)}{k_p} + \frac{\ln(r_f/r_p)}{k_f}\right) = 5.0\ \text{K/W} \tag{1}$$

$$R_y = \frac{l_p}{k_p A_p} = \frac{l_p}{k_p \pi \cdot r_p^2} = 200.9\ \text{K/W} \tag{2}$$

where r_p, l_p, A_p and k_p are the radius, length, cross-sectional area and thermal conductivity of the piezoelectric stack, respectively. k_f represents the thermal conductivity of the packaging housing. The values of r_p, l_p, A_p are listed in Table 1 and the values of k_p, k_f are listed in Table 2. The results show that the radial thermal resistance is much less than the axial thermal resistance. In addition, the boundary condition of the piezoelectric stack is a constant heat flux rather than convective heat transfer. Therefore, the radial temperature gradient of the piezoelectric stack is much smaller than the axial temperature gradient, which means that the radial temperature variation can be negligible[21].

Table 1 Relevant dimension parameters of structure

Parameter	Description	Value
r_p / m	Radius of the piezoelectric stack	6.5×10^{-3}
A_p / m^2	Cross-sectional area of the piezoelectric stack	1.33×10^{-4}
l_p / m	Length of the piezoelectric stack	0.04
r_f / m	Radius of the packaging housing	7.5×10^{-3}
A_f / m^2	Cross-sectional area of packaging housing	4.39×10^{-5}
l_f / m	Length of the packaging housing	0.047
P / m	Perimeter of the packaging housing	0.047
A_h / m^2	Area of the heating film	2.2×10^{-3}
A_{hb} / m^2	Area of the bottom of the packaging housing	1.77×10^{-4}
r_m / m	Radius of the mechanical structure	3.2×10^{-2}
A_m / m^2	Area of the mechanical structure	3.2×10^{-3}
l_m / m	Thickness of the mechanical structure	1.6×10^{-2}

Table 2 The thermophysical properties

Parameter	Description	Value
T_0 / ℃	External environment temperature	-70
h_0 / (W·(m^2·K)$^{-1}$)	Heat transfer coefficient	60
k_p / (W·(m·K)$^{-1}$)	Thermal conductivity of the piezoelectric stack	1.5
k_f / (W·(m·K)$^{-1}$)	Thermal conductivity of the packaging housing	16.2
k_m / W·(m·K)$^{-1}$)	Thermal conductivity of the mechanical structure	10
R_c / (m^2·K·W^{-1})	Thermal contact resistance per unit area	5.8×10^{-4}

Then, the simplifying assumptions can be summarized as:

(1) The steady state conduction is achieved.

(2) The temperature of cross section in the axial direction is uniform.

(3) All the properties of materials remain constant.

The heat conduction in the axial direction of the piezoelectric stack can be simplified to a one-dimensional heat conduction, and the thickness of the packaging housing is sufficiently small (1 mm) so that the temperatures of the packaging housing and the piezoelectric stack remain unchanged in the same cross section. Therefore, the packaging housing (in the black dotted rectangle in Fig.2) as the analysis object, the micro-element of length dy is adopted as the control volume. As shown in Fig.3, the energy balance equation is

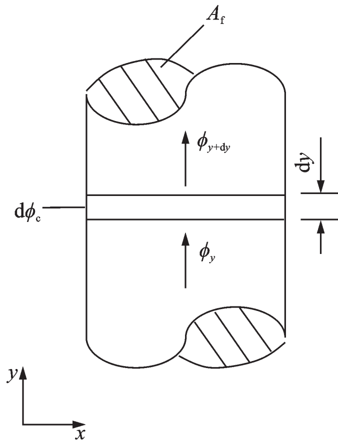

Fig.3 Schematic drawing of the energy balance

$$\phi_y + \mathrm{d}\phi_c = \phi_{y+\mathrm{d}y} \tag{3}$$

where ϕ_y and $\phi_{y+\mathrm{d}y}$ are the heat transfer that enters into and dissipates from the control volume, respectively; dϕ_c represents the constant heat transfer at the boundary of the control volume. According to the Fourier's law[22], the corresponding components can be expressed as

$$\phi_y = -k_f A_f \frac{\mathrm{d}T}{\mathrm{d}y} \tag{4}$$

$$\phi_{y+\mathrm{d}y} = \phi_y + \frac{\mathrm{d}\phi_y}{\mathrm{d}y}\mathrm{d}y \tag{5}$$

$$\mathrm{d}\phi_c = q \cdot \mathrm{d}A_h \tag{6}$$

where T is the temperature, q the heat flux, A_h and A_f the area of the heating film and the cross-sectional area of packaging housing, respectively. Substituting Eqs.(4)—(6) into Eq.(3), the energy balance equation can be written as

$$k_f A_f \frac{\mathrm{d}^2 T}{\mathrm{d}y^2} + q\frac{\mathrm{d}A_h}{\mathrm{d}y} = 0 \tag{7}$$

The perimeter of the heating film is P, then d$A_h = P$dy, thus Eq.(7) can be further simplified as

$$\frac{\mathrm{d}^2 T}{\mathrm{d}y^2} + \frac{qP}{k_f A_f} = 0 \tag{8}$$

Considering the constant $n = qP/k_f A_f$, Eq.(8) can be written as

$$\frac{\mathrm{d}^2 T}{\mathrm{d}y^2} + n = 0 \tag{9}$$

The two boundary conditions are

$$y = 0, T = T_b; y = l_p, \mathrm{d}T/\mathrm{d}y = 0 \tag{10}$$

where T_b is the temperature at the bottom of the piezoelectric stack.

According to the above derivation, the temperature distribution function of piezoelectric stack in the axial direction can be solved from Eqs.(9) and (10).

$$T(y) = -\frac{n^2}{2}y^2 + nl_p y + T_b \tag{11}$$

The heat flux q is determined based on its concept

$$q = \frac{Q}{A_h} = \frac{Q}{P \cdot l_f} = \frac{Q}{2\pi \cdot r_f \cdot l_f} \tag{12}$$

where l_f is the length of the packaging housing, Q the heat generated by the heating film, and thus the constant n can be solved. Besides, the only unknown parameter in the temperature distribution function (Eq.(11)) is the temperature value T_b.

Since the bottom of packaging housing with small size is also covered by the heating film, it can be claimed that the bottom temperature of the packaging housing is equal to the bottom of the piezoelectric stack T_b. As shown in Fig.4, the heat is transferred to external environment through the mechanical structure.

Here, T_0 is the temperature of external environment with heat transfer coefficient h_0. T_m is the temperature at the top of the mechanical structure, which is lower than T_b because of the thermal contact resistance between the two different structures.

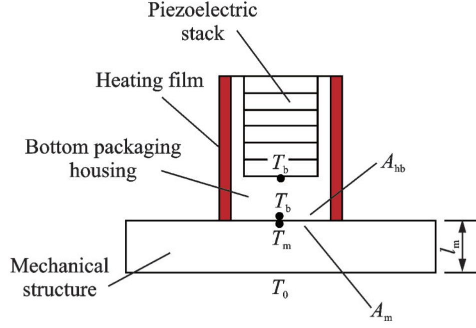

Fig.4 Schematic diagram of heat conduction of the structure bottom

Based on the concept of the thermal contact resistance per unit area R_c [23], the heat conduction formula through the thermal contact resistance is obtained as

$$Q = A_{hb}\frac{T_b - T_m}{R_c} = \pi \cdot r_f^2 \cdot \frac{T_b - T_m}{R_c} \tag{13}$$

where A_{hb} is the area of the bottom packaging housing. The heat conduction formula through the mechanical structure is obtained as follows, which is regarded as the one-dimensional steady-state conduction through the plane wall.

$$Q = A_m \frac{T_m - T_0}{\frac{1}{h_0} + \frac{l_m}{k_m}} = \pi \cdot r_m^2 \cdot \frac{T_m - T_0}{\frac{1}{h_0} + \frac{l_m}{k_m}} \tag{14}$$

where A_m, r_m, k_m and l_m are the area, radius, thermal conductivity and thickness of the mechanical structure, respectively. Then the temperature value T_b can be calculated in a combination of Eqs.(13) and (14).

$$T_b = \frac{(k_m + h_0 l_m)Q}{h_0 k_m \pi r_m^2} + \frac{QR_c}{\pi r_f^2} + T_0 \tag{15}$$

Parameters mentioned above are listed in Table 1.

The packaging housing is made of stainless steel, so the thermal contact resistance per unit area R_c can be calculated according to the empirical value between stainless steel at normal pressure and surface roughness[24]. The mechanical is made of Invar with low thermal expansion to accommodate cryogenic temperature. The thermal conductivity of the piezoelectric stack k_p can be obtained from the company's product manual. The low temperature test chamber used for testing whose available lowest temperature T_0 is 70 ℃. That is to say, under that circumstance the convective heat transfer is forced convection, and the heat transfer coefficient h_0 can be determined according to the empirical value[23]. Relevant thermophysical properties mentioned above are listed in Table 2.

When the thermal power of heating film Q is 2.7 W, the bottom temperature of the stack $T_b = -45.8$ ℃, which can be obtained on the basis of Eq.(15), then the axial temperature distribution of piezoelectric stack can be obtained by substituting the bottom temperature T_b into Eq.(11), as shown in Fig.5.

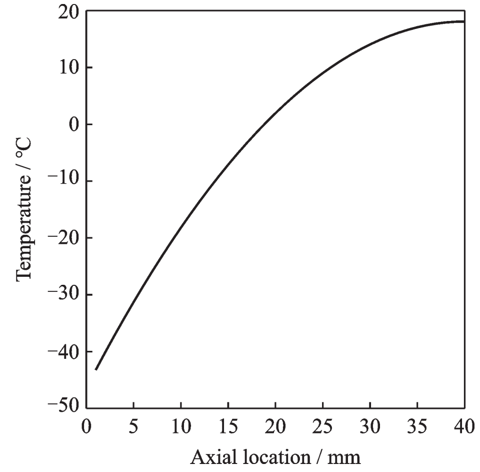

Fig.5 Temperature distribution of piezoelectric stack in the axial direction under whole heating condition

It can be inferred that the axial temperature gradient is quite large under overall heating condition, with the maximum temperature difference of 61 ℃, which may be harmful to itself.

(1) Different degrees of thermal expansion and change of the preloading force will be triggered due to the large temperature gradient which will further impose great impact on its driving capability ultimately.

(2) The gradient distribution of the piezoelectric constant will be present in the axial direction, which is influential to the driving capability as well.

1.2.2 Local heating theoretical analysis

Since the heat loss mainly comes from the bottom of the piezoelectric stack, for the purpose of reducing the temperature gradient, it is considered to adopt a local heating method, which means that the heating film covers only the bottom of the piezoelec-

tric stack. The length of the heating film is H, and the length of the heating film covering area is H_p.

Similarly, based on the above three simplifying assumptions, it is assumed that the temperatures of the package housing and the piezoelectric stack are equal in the same cross section. The packaged housing cover by the heating film (in the black dotted rectangle) is selected as the analysis object.

The piezoelectric stack is divided into a heating section ($0\leqslant y\leqslant H_p$) and an unheated section ($H_p< y\leqslant l_p$) as shown in Fig.6.

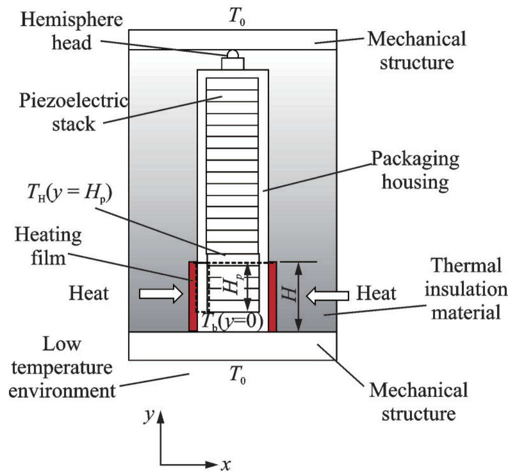

Fig.6 Local heating thermal conductivity model

The heat conduction equation is the same as Eq.(9), but the boundary conditions in the heating section are different.

$$\frac{d^2T}{dy^2}+n=0 \tag{16}$$

$$y=0,\ T=T_b;\ y=H_p,\ T=T_H \tag{17}$$

Then the temperature distribution function of piezoelectric stack in the axial direction can be solved from Eqs.(16) and (17).

$$T(y)=-\frac{ny^2}{2}+\left(\frac{T_H-T_b}{H_p}+\frac{nH_p}{2}\right)y+T_b \quad 0\leqslant y\leqslant H_p \tag{18}$$

The heat flux q can be determined as

$$q=\frac{Q}{A_h}=\frac{Q}{P\cdot H}=\frac{Q}{2\pi\cdot r_f\cdot H} \tag{19}$$

When $H_p<y\leqslant l_p$, the energy balance equation is as follows

$$\phi_y=\phi_{y+dy} \tag{20}$$

By substituting Eqs.(4) and (5) into the energy balance Eq.(20), the heat conduction equation in the unheated section can be obtained as

$$\frac{d^2T}{dy^2}=0 \tag{21}$$

The boundary conditions are

$$y=H_p, T=T_H; y=l_p, \frac{dT}{dy}=0 \tag{22}$$

The temperature distribution function in the axial direction can be solved from Eqs.(21) and (22).

$$T(y)=T_H, H_p<y\leqslant l_p \tag{23}$$

Eq.(23) shows that temperature distribution is uniform in the unheated section, and the temperature value is equal to the temperature of T_H. Therefore, the temperature distribution function can be solved by the calculation of T_H and T_b.

According to the Fourier's law, the heat of the heating section can be obtained from Eq.(18).

$$Q(y)=-k_pA_p\frac{dT}{dy}=-k_pA_p\left(-ny+\frac{T_H-T_b}{H_p}+\frac{nH_p}{2}\right) \tag{24}$$

When $y=H_p$, the heat is

$$Q(H_p)=-k_pA_p\left(-\frac{nH_p}{2}+\frac{T_H-T_b}{H_p}\right) \tag{25}$$

Since the temperature in the unheated section is uniform, namely the temperature gradient and the heat input in this section are zero, Eq.(25) can be set to 0.

$$-k_pA_p\left(-\frac{nH_p}{2}+\frac{T_H-T_b}{H_p}\right)=0 \tag{26}$$

$$T_H=\frac{1}{2}(H_p^2n+2T_b) \tag{27}$$

The whole generated heat is transferred to the external environment through the bottom of the stack due to the fact that the heat input in unheated section is zero, so the temperature value T_b can be calculated by Eq.(15) as well. In consequence, the axial temperature distribution of the stack under local heating condition can be acquired by substituting the temperature value T_H and T_b into Eqs.(18) and (23).

It is further necessary to determine the power and size of the heating film so that the piezoelectric stack can satisfy the following requirements: (1) Its temperature is higher than 0 ℃; (2) the axial tem-

perature gradient is small.

With regard to the size of the heating film, the width is determined by the perimeter of the piezoelectric stack. According to the result of the whole heating theoretical model, it can be inferred that under the constant heating power, the smaller the length of the heating film is, the smaller the stack temperature gradient is. Through the investigation, the length of the heating film H is 10 mm, which is the minimum size of heating film available in the market, and the thickness of the bottom packaging housing is measured as 4 mm, so the length of the heating section H_p is 6 mm.

Regarding the power of the heating film, for the reason that the bottom temperature of piezoelectric stack descends to its lowest point on the basis of the calculated results, the whole temperature of the stack should be higher than 0 ℃ provided that the bottom temperature is higher than 0 ℃. Taking the temperature value at the height of 1 mm, the power is 7.2 W, which can ensure that the bottom temperature is not lower than 0 ℃ by setting the $T(0.001)=0$ ℃. The heating power is set to $Q\geqslant 7.3$ W in practice.

According to the two temperature distribution Eqs.(18) and (23), the temperature gradient only exists in the heating section, and the temperature difference between two ends of the heating section is the maximum. Therefore, by calculating temperatures at the height of 1 mm and 6 mm, we can acquire the minimum temperature difference ($\Delta T_{min}=$ 12.8℃) when the heating power is the minimum value ($Q=7.3$ W). In conclusion, when the heating power Q and the length H of heating film are 7.3 W and 10 mm respectively, a minimum temperature gradient of the piezoelectric stack can be attained, which is satisfying. The axial temperature distribution of piezoelectric stack is shown in Fig.7.

Comparing two heating modes, as shown in Fig. 8 and Table 3, it can be conclude that, after adopting the local heating mode, the maximum temperature difference of the stack can be reduced by 80%, and the two requirements mentioned above can be achieved.

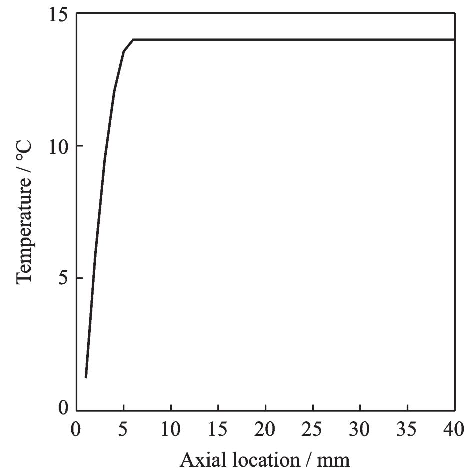

Fig.7 Temperature distribution of piezoelectric stack in the axial direction under local heating condition

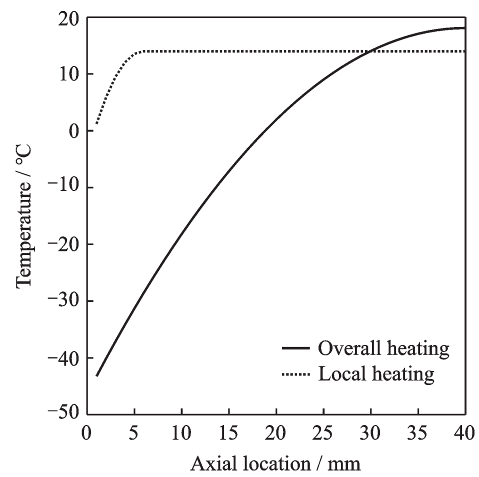

Fig.8 Comparison of the axial temperature distribution of piezoelectric stack under two heating conditions

Table 3 Comparison of two heating modes ℃

Temperature	Overall heating	Local heating
The maximum temperature	18.7	13.0
The minimum temperature	−42.6	0.9
The maximum temperature difference	61.3	12.1

2 Experiments

2.1 Experimental setup

For the sake of verifying the effectiveness of the heating and insulation structure, it is part and parcel to measure the temperature as well as the properties of the piezoelectric stack. To be exact, the electromechanical properties of the piezoelectric stack are described by three sets of matrix coefficient values describing the piezoelectric, dielectric

and elastic properties of the stack[7]. A piezoelectric stack produced by Harbin Core Tomorrow Science and Technology Co., Ltd, is put to use in this experiment, which is a conventional piezoelectric stack with a packaging housing (PSt 150/10×10/20), as shown in Fig.9.

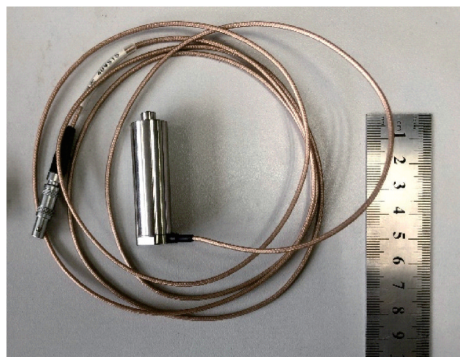

Fig.9 Conventional piezoelectric stack used in the experiment

In addition, an impedance analyzer (ZX80A-5M) manufactured by Changzhou Zhixin Precision Electronics Co., Ltd, a low-temperature test chamber (HRH0270type) and a temperature sensor (WZP) are adopted. The conventional piezoelectric stack pasted by a heating film (HXDR-PI) at the bottom is installed inside of the mechanical structure. In detail, the rated power of the heating film which is made of polyimide is 10 W, and the resistance is 30 Ω. What's more, two thermocouple probes, which are connected by two digital multimeters (LINI-T UT71C and FLUKE 17B), are installed at the top and bottom of the packaging housing respectively to measure the temperature at both ends, as shown in Fig.10. Then the stack, wrapped by a layer of thermal insulation material as described before, is connected to the impedance analyzer. Furthermore, the mechanical structure is pasted with a temperature sensor to measure its surface temperature. All data cables connect the internal measured stack with the external instruments through the hole at the side of the test chamber. Fig.11 displays the experimental arrangements in

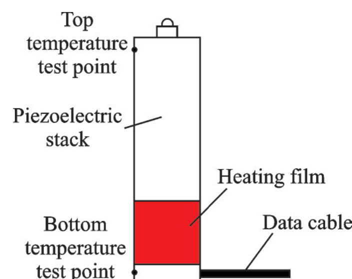

Fig.10 Diagram of piezoelectric stack temperature test

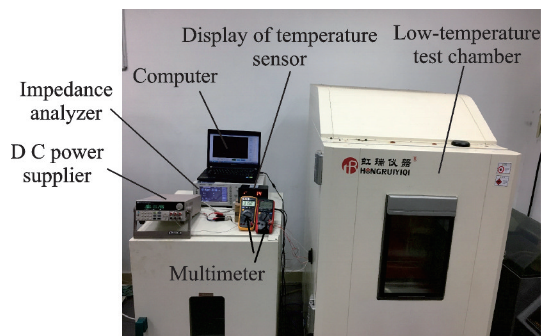

(a) Overall photograph of the experimental devices

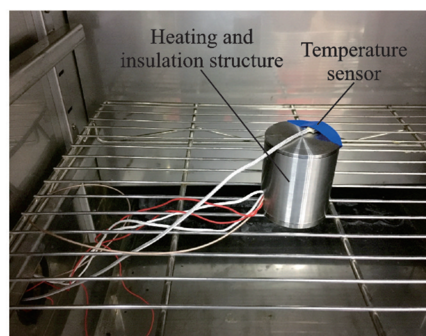

(b) Photograph inside the test chamber

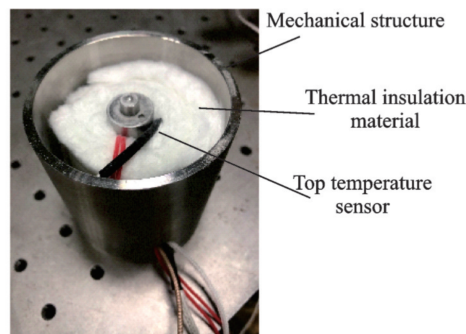

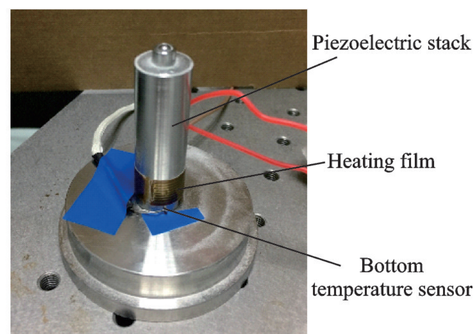

(c) Photograph inside heating and insulation structure

Fig.11 Display of the experimental devices

detail.

For further research, it is significant to compare the experimental results with and without the warming structure, while the used conventional piezoelectric stack will sustain a damage when it is directly exposed to cryogenic environment. Therefore, another low-temperature-resistant piezoelectric stack without a packaging housing (Harbin Core Tomorrow Science and Technology Co., Ltd. PSt 150/20) which can be exposed to low temperature is employed in the experiment without the warming structure, as shown in Fig.12.

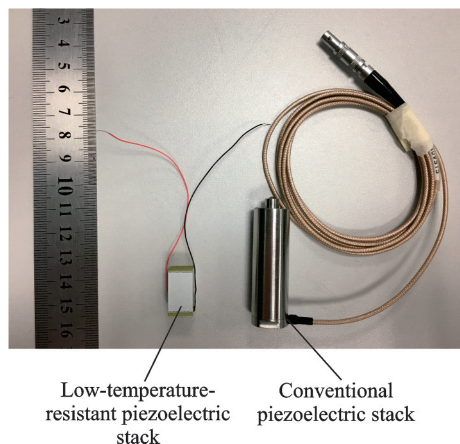

Fig.12 Two kinds of piezoelectric stacks

Additionally, the materials of the two stacks are exactly the same so that the properties including piezoelectric constant, elastic compliance, relative dielectric constant and electromechanical coupling coefficient could be compared, which can guarantee the validity of the comparison of the results.

As described before, the low-temperature-resistant piezoelectric stack is put in the low-temperature test chamber, and then the impedance analyzer and the temperature sensor are utilized to test its properties and surface temperature separately. The piezoelectric stack is connected to the impedance by the cable which is packaged with the thermal insulation material to protect it from the low temperature. The experimental facilities are shown in Fig.13.

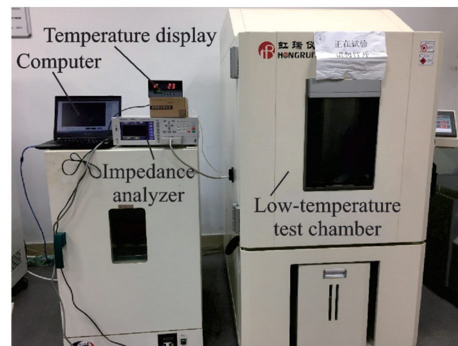

(a) External overall layout of the experiment

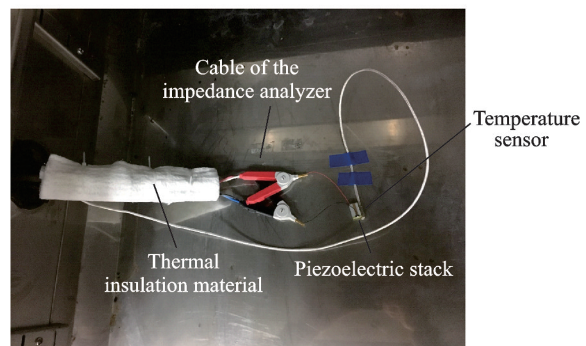

(b) Setup inside the test chamber

Fig.13 Experimental setup without the warming structure

2.2 Experimental results and discussion

2.2.1 Temperature testing results

In the experiment, four different temperatures are measured varying with time, including the bottom and top temperatures of the conventional piezoelectric stack, the surface temperature of the mechanical structure as well as the ambient temperature. Specifically, the ambient temperature inside the chamber could be reduced from 20 ℃ to −70 ℃ by control and then maintained at −70 ℃ for 1 h in order to reach the steady-state conduction. The heating film generates the heat increasing gradually as the ambient temperature declines by adjusting the excitation voltage of the DC power supply (IT6302), in order to keep stack's temperature as steady as possible. As for the heating power of the heating film, it is maintained at 7.3 W eventually in line with the results of theoretical analysis. Each temperature value is recorded at every two-minute interval during the decline of ambient temperature, as shown in Fig.14.

It can be inferred that the surface temperature of the mechanical structure drops along with the decrease in the ambient temperature. Meanwhile, the

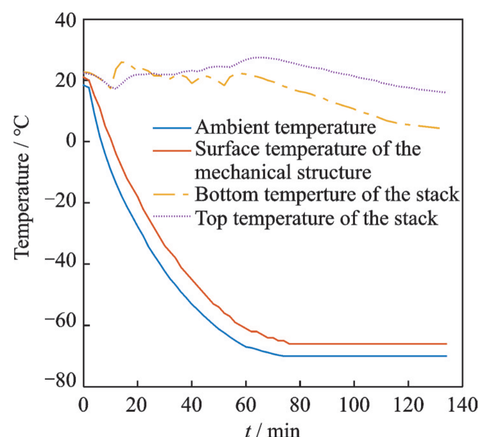

Fig.14 Comparison of the four different temperatures variation with time

top and bottom temperatures of the piezoelectric stack, however, are almost stable. The bottom temperature drops a little due to more heat loss at the bottom but it is still above 0 ℃, which proves that the temperature of piezoelectric stack can remain normal under low temperature environment. Besides, it is clear from Fig.14 that the temperature of the piezoelectric stack could still be maintained normal for a long time after that the ambient temperature has dropped to −70 ℃, which could reflect the thermal stability of the warming structure.

The comparison between the theoretical and experimental results of the top and bottom temperatures of piezoelectric stacks, as shown in Table 4, indicates that as far as the temperature at both ends of the stack is concerned, the theoretical results are consistent with the experimental ones with a maximum temperature difference of 3.4 ℃.

Table 4 Comparison between the theoretical and experimental results ℃

Temperature	Theoretical results	Experimental results	Difference between theoretical and experimental results
Top temperature	13.0	16.0	3
Bottom temperature	0.9	4.3	3.4

In consequence, the consistency between the measurement results and theoretical results has verified the correctness of the theoretical analysis.

2.2.2 Properties measurement

The elastic, dielectric, and piezoelectric coefficients of piezoelectric ceramics are determined by the resonance method, outlined in the IEEE Standard 176[25] which is able to determine the material properties of piezoelectric stack as well[22]. The range of testing frequency, including the fundamental resonance frequency f_r and anti-resonant frequency f_a of the stack, is 10—26 kHz. With the change of the ambient temperature at which the resonance measurement is taken, the properties of the piezoelectric stack are calculated through the following equations[26].

$$s_{33}^{E}=\frac{1}{4\rho\cdot f_r^{2}\cdot(t_p n)^2} \tag{28}$$

$$\varepsilon_{33}^{T}=\frac{C^{T}t_p}{nA_P} \tag{29}$$

$$\frac{K_{33}^2}{1-K_{33}^2}=\frac{\pi}{2}\cdot\frac{f_a}{f_r}\tan\left(\frac{\pi}{2}\cdot\frac{f_a-f_r}{f_r}\right) \tag{30}$$

$$d_{33}=K_{33}\cdot\sqrt{\varepsilon_{33}^{T}\cdot s_{33}^{E}} \tag{31}$$

where s_{33}^{E} is the elastic compliance, ε_{33}^{T} the relative dielectric constant, K_{33} the electromechanical coupling coefficient, and d_{33} the piezoelectric constant. The other relevant parameters are listed in Table 5. The temperature dependence of the properties can be determined through experiments and the results are as demonstrated in Figs.(15—18).

Table 5 Parameters of piezoelectric stacks

Parameter	Description	Values of the conventional piezoelectric stack	Values of the low-temperature-resistant piezoelectric stack
n	Layer number	400	180
t_p / μm	Thickness	1.0×10^{-4}	
ρ / (kg·m^{-3})	Density	8 333	
A_p / m^2	Cross-sectional area	1.33×10^{-4}	1.00×10^{-4}

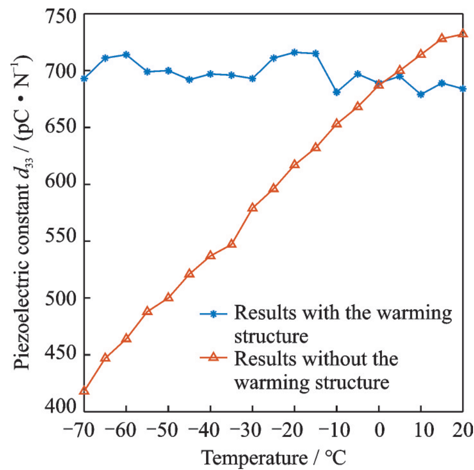

Fig.15 Comparison of the temperature dependence of the piezoelectric constant with or without the warming structure

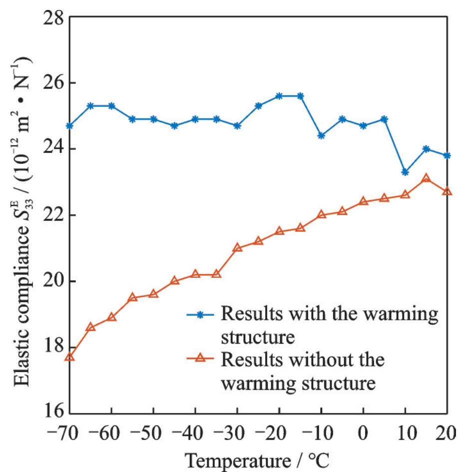

Fig.16 Comparison of the temperature dependence of the elastic compliance with or without the warming structure

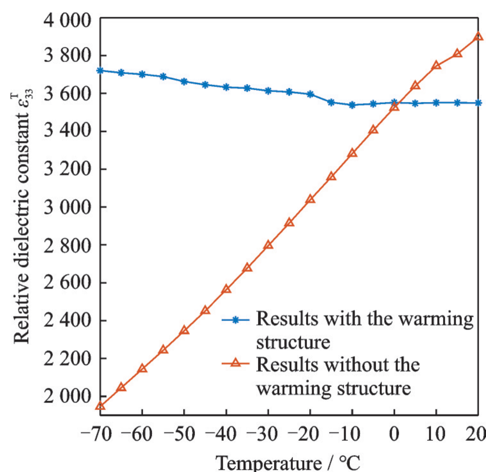

Fig.17 Comparison of the temperature dependence of the relative dielectric constant with or without the warming structure

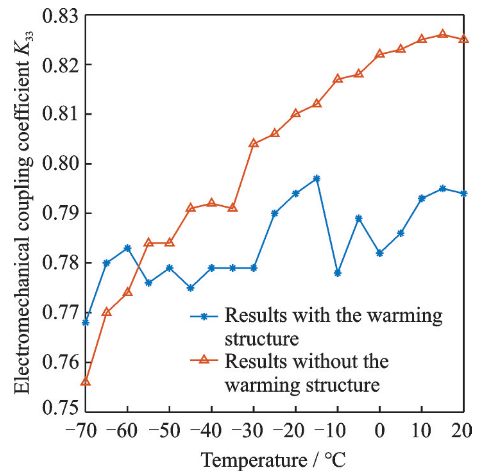

Fig.18 Comparison of the temperature dependence of the electromechanical coupling coeffcient with or without the warming structure

It can be observed that when the piezoelectric stack is installed with the warming structure, the properties are almost invariable and not affected by the ambient temperature drop, which verifies the feasibility of the heating and insulation structure within the range from normal temperature to −70 ℃. Relatively speaking, the properties all decrease 40% approximately as the ambient temperature declines when the piezoelectric stack is directly exposed to low temperature environment, which has been mutually verified with Ref.[27]. According to the local heating thermal conductivity model, the size and heating power of a heating film can be estimated and chosen on account of such factors as the ambient temperature, heat transfer coefficient as well as the required temperature of the piezoelectric stack, etc. Consequently, this heating and insulation method could be universally adapted and is also applicable for other ambient temperature conditions, so long as some essential adjustments of design are made. On the aforementioned basis, it is imperative to continue developing a warming structure that is applicable in lower temperature environment using a chamber cooled by liquid nitrogen in recent future.

3 Conclusions

A warming structure for the piezoelectric stack applied in low temperature has been successfully de-

signed in this paper. Thermal conductivity models under two different heating modes are analyzed and validated by testing as well. In addition, heating and insulation experiments have been conducted to measure the variation of the temperature and the properties of piezoelectric stack with ambient temperature drop and the experiment without the warming structure performed for comparative purposes. In conclusion, the results reveal that the theoretical analysis are consistent with the experimental results closely. Furthermore, the properties are kept stable for a long period of time as temperature varying from normal temperature to −70 ℃, which confirms the effectiveness and reliability of the structure. Consequently, the design philosophy has highly significant reference under different temperatures. In short, this structure can be popularized and widely implemented in lower temperature environments.

References

[1] GU G Y, ZHU L M, SU C Y. Modeling and compensation of asymmetric hysteresis nonlinearity for piezoceramic actuators with a modified Prandtl-Ishlinskii model[J]. IEEE Transactions on Industrial Electronics, 2014, 61(3): 1583-1595.

[2] HAN C, JEON J, CHUNG J U, et al. Dynamic characteristics and control capability of a piezostack actuator at high temperatures: Experimental investigation[J]. Smart Materials and Structures, 2015, 24(5): 057002.

[3] KORUZA J, FRANZBACH D J, SCHADER F, et al. Enhancing the operational range of piezoelectric actuators by uniaxial compressive preloading[J]. Journal of Physics D Applied Physics, 2015, 48(21): 215302.

[4] LI F X, RAJAPAKSE R K N D, MUMFORD D, et al. Quasi-static thermo-electro-mechanical behaviour of piezoelectric stack actuators[J]. Smart Materials and Structures, 2008, 17(1): 015049.

[5] GU G Y, ZHU L M. Comparative experiments regarding approaches to feedforward hysteresis compensation for piezoceramic actuators[J]. Smart Materials and Structures, 2014, 23(9): 095029.

[6] ISLAM M N, SEETHALER R, ALAM M S. Characterization of piezoelectric materials for simultaneous strain and temperature sensing for ultra-low frequency applications[J]. Smart Materials and Structures, 2015, 24(8): 085019.

[7] LI Y, SHEN X, CHEN Y C. Design, experiment and verification of a refined resonance method for property measurement of piezoelectric stack[J]. Smart Materials and Structures, 2019, 28(1): 015033.

[8] ZENKOUR A M, AREFI M. Nonlocal transient electrothermomechanical vibration and bending analysis of a functionally graded piezoelectric single-layered nanosheet rest on visco-Pasternak foundation[J]. Journal of Thermal Stresses, 2016, 40(2): 1-18.

[9] WANG Liwei, XIA Pinqi. Active vibration isolation of helicopter by using piezoelectric stack actuators installed on struts of main gearbox[J]. Journal of Nanjing University of Aeronautics & Aeronautics, 2018, 50(2): 233-238. (in Chinese)

[10] ZHANG X, ZHAO G F, PAN M, et al. The research of piezoelectric actuator for cryogenic scanning application[C]//Proceedings of International Symposium on Photoelectronic Detection and Imaging. Beijing: [s.n.], 2011: 819332.

[11] FEHREN H, GNAUERT U, WIMMEL R, et al. Validation testing with the active damping system in the European transonic wind tunnel[C]//Proceedings of the 39th AIAA Aerospace Sciences Meeting and Exhibit. Reno: AIAA, 2001: 610.

[12] BALAKRISHNA S, BUTLER D, WHITE R, et al. Active damping of sting vibrations in transonic wind tunnel testing[C]//Proceedings of AIAA Aerospace Sciences Meeting and Exhibit. [S.l.]: AIAA, 2008: 840.

[13] BALAKRISHNA S, BUTLER D, ACHESON M, et al. Design and performance of an active sting damper for the NASA common research model[C]//Proceedings of the 49th AIAA Aerospace Sciences Meeting Including the New Horizons Forum and Aerospace Exposition. Orlando: AIAA, 2011: 953.

[14] SHINDO Y, NARITA F. Piezomechanics in PZT stack actuators for cryogenic fuel injectors[J]. Smart Actuation and Sensing Systems-Recent Advances and Future Challenges, 2012, 22(5): 638-656.

[15] GAO X Y, YAN Y K, CARAZO A V, et al. Low-temperature Co-fired unipoled multilayer piezoelectric transformers[J]. IEEE Transactions on Ultrasonics Ferroelectrics & Frequency Control, 2017, 65(3): 513-519.

[16] TANG L, TIAN H, ZHANG Y, et al. Temperature dependence of dielectric, elastic, and piezoelectric constants of [001]_c poled Mn-doped 0.24Pb (In_(1/2) Nb_(1/2)) O_3-0.46Pb(Mg_(1/3) Nb_(2/3)) O_3-0.30PbTiO_3 single crystal[J]. Applied Physics Letters, 2016, 108(8): 082901.

[17] SABAT R G, MUKHERJEE B K, REN W, et al. Temperature dependence of the complete material coefficients matrix of soft and hard doped piezoelectric lead zirconate titanate ceramics[J]. Journal of Applied Physics, 2007, 101(6): 121-126.

[18] SENOUSY M S, RAJAPAKSE R K N D, MUMFORD D, et al. Self-heat generation in piezoelectric stack actuators used in fuel injectors[J]. Smart Materials and Structures, 2009, 18(4): 045008.

[19] RIVERS M B, BALAKRISHNA S. NASA common research model test envelope extension with active sting damping at NTF[C]//Proceedings of AIAA Applied Aerodynamics Conference. Atlanta: AIAA, 2014: 3135.

[20] ZHANG Jingzhou, CHANG Haiping. Heat transfer (2nd edition)[M]. Beijing: Science Publishing, 2009: 33-67. (in Chinese)

[21] ZHANG Jingzhou. Advanced heat transfer (2nd edition)[M]. Beijing: Science Publishing, 2015: 58-73. (in Chinese)

[22] SHERRIT S, LEARY S P, BAR-CHEN Y, et al. Analysis of the impedance resonance of piezoelectric stacks[C]//Proceedings of 2000 IEEE Ultrasonics Symposium. Puerto Rico: IEEE, 2000: 1037-1040.

[23] INCROPERA F P, DEWITT D P. Fundamentals of heat and mass transfer[M]. Beijing: Chemical Industry Publishing, 2007: 67-81.

[24] TAO Wenquan. Heat transfer[M]. Xi'an: Northwestern Polytechnical University Publishing, 2006: 39-54. (in Chinese)

[25] MEITZLER A H, BERLINCOURT D, WELSH F S, et al. IEEE standard on piezoelectricity[C]//Proceedings of ANSI/IEEE Std 176—1987. New York: IEEE, 1987: 46-63.

[26] SHERRIT S, DAPINO M J, OUNAIES Z, et al. Multilayer piezoelectric stack actuator characterization[J]. Behavior and Mechanics of Multifunctional and Composite Materials, 2008, 6929(1): 692909.

[27] SHEN Xing, LI Yang, LIANG Lei, et al. Self-sensing test method for the temperature of piezoelectric stacks[J]. Transactions of Nanjing University of Aeronautics and Astronautics, 2019, 36(1): 109-118.

Acknowledgements This work was supported by the National Natural Science Foundation of China (No. 11872207), the Aeronautical Science Foundation of China (No. 20180952007), the Research Fund of State Key Laboratory of Mechanics and Control of Mechanical Structures (No. MCMS-I-0520G01), and the Key Laboratory Foundation of Equipment Pre-Research (No. 6142204200307).

Authors Ms. **LIN Yufan** received her B.S. degree in aerocraft design from Nanjing University of Aeronautics and Astronautics(NUAA) in 2018, and joined the State Key Laboratory of Mechanics and Control of Mechanical Structures as a postgraduate student. Her main research field is smart materials and structures.

Prof. **SHEN Xing** received the Ph.D. degree from NUAA in 2003. He is now a professor of NUAA. His research is focused on Aeronautical smart structure, which includes design and test of the piezoelectric ceramics, piezoelectric sensors and actuators and relative research in the smart materials and structures.

Author contributions Ms. **LIN Yufan** complied the theoretical model, conducted the analysis, completed the tests and wrote the manuscript. Dr. **QIN Xuguo** contributed to the investigation of the study. Mr. **YU Yi** assisted with theoretical analysis and revision of the manuscript. Prof. **SHEN Xing** designed the study, reviewed the manuscript and provided advices. All authors commented on the manuscript draft and approved the submission.

Competing interests The authors declare no competing interests.

(Production Editor: WANG Jing)

一种低温下压电叠堆保温结构研究

林俞帆[1]，秦绪国[2]，于　艺[1]，樊思昀[1]，沈　星[1]

（1.南京航空航天大学机械机构力学及控制国家重点实验室，南京 210016，中国；2.北京航天长征飞行器研究所，北京 100076，中国）

摘要：目前研究表明压电叠堆的性能会随着温度降低而下降，这种现象会对其在低温环境下的应用产生负面影响。为了解决这个问题，本文提出了一种便捷且有效的压电叠堆保温结构。本文首先通过热传递理论分析，对整体和局部这两种加热方式进行了分析和比较，其次进一步通过实验评估保温结构的有效性。实验表明，理论分析与实验结果一致，并且当温度从10 ℃下降至－70 ℃时，压电叠堆的温度和性能保持稳定，证明了保温结构的可行性。因此，本文可以为从事智能材料和结构的低温研究的人员提供参考。

关键词：保温结构；压电叠堆；低温；热传递